BB

LBL-35290
UC-413
Preprint

Lawrence Berkeley Laboratory
UNIVERSITY OF CALIFORNIA

Submitted to Physical Review C

β^+ Decay and Cosmic-Ray Half-Lives of ^{143}Pm and ^{144}Pm

M.M. Hindi, A.E. Champagne, M.T.F. da Cruz, R.M. Larimer,
K.T. Lesko, E.B. Norman, and B. Sur

February 1994

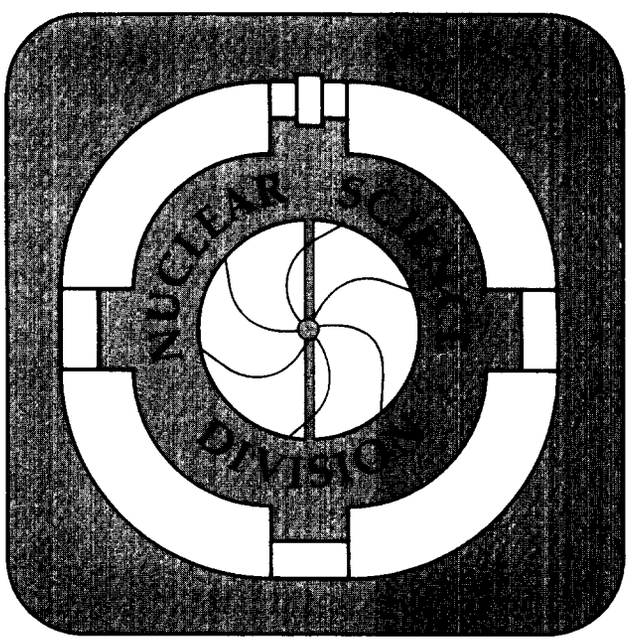

Prepared for the U.S. Department of Energy under Contract Number DE-AC03-76SF00098

LBL - 35290

β^+ Decay and Cosmic-Ray Half-Lives of ^{143}Pm and ^{144}Pm

M.M. Hindi,(1), A.E. Champagne,(2) M.T.F. da Cruz,(3)
R.M. Larimer,(3) K.T. Lesko, (3) E.B. Norman,(3) and B. Sur,(3)

(1)Physics Department, Tennessee Technological University, Cookeville, TN 38505
(2) Department of Physics and Astronomy, University of North Carolina at Chapel Hill, Chapel Hill, North Carolina 27599
(3) Nuclear Science Division, Lawrence Berkeley Laboratory, Berkeley, CA 94720

Nuclear Science Division, Lawrence Berkeley Laboratory
University of California, Berkeley, California 94720, USA

February 22, 1994

This work was supported by the Director, Office of Energy Research Division of Nuclear Physics of the Office of High Energy and Nuclear Physics of the U.S. Department of Energy under Contract DE-AC03-76SF00098

β^+ decay and cosmic-ray half-lives of ^{143}Pm and ^{144}Pm

M. M. Hindi,[1] A. E. Champagne,[2] M. T. F. da Cruz,[3]* R.-M. Larimer,[3] K. T. Lesko,[3] E. B. Norman,[3] and B. Sur,[3]†

[1] *Physics Department, Tennessee Technological University, Cookeville, Tennessee 38505*

[2] *Department of Physics and Astronomy, University of North Carolina at Chapel Hill, Chapel Hill, North Carolina 27599*

[3] *Nuclear Science Division, Lawrence Berkeley Laboratory, Berkeley, California 94720*

(February 22, 1994)

Abstract

The positron decay partial half-lives of ^{143}Pm and ^{144}Pm are needed to assess the viability of elemental Pm as a cosmic-ray clock. We have conducted experiments to measure the β^+ branches of these isotopes; we find β^+ branches of $< 5.7\times10^{-6}$% for ^{143}Pm and $< 8\times10^{-5}$% for ^{144}Pm. Although these branches are a factor of 20 lower than the previous experimental limits, the resulting partial half-lives are still too uncertain to permit any firm conclusions.

PACS Numbers: 23.40.-s, 27.60.+j, 96.40.De

Typeset using REVTEX

---

*Permanent address: Physics Institute, University of São Paulo, São Paulo, Brazil.

†Present address: Atomic Energy of Canada Limited Research, Chalk River Laboratories, Chalk River, Ontario K0J 1J0, Canada.

I. INTRODUCTION

The mean confinement time of cosmic rays within the Galaxy can be determined by comparing the cosmic-ray abundances of suitably long-lived radioactive isotopes to their stable neighbors. For heavy elements ($Z \geq 28$) the current state of the art in cosmic-ray mass measurement is not sufficient to resolve a radioactive isotope from its immediate neighbor. This difficulty prompted Drach and Salamon [1] to consider the possibility of using the elemental abundances of Tc and Pm, which have no stable isotopes, as cosmic-ray clocks. They were able to make reasonable estimates of the cosmic-ray half-lives of ^{95}Tc and ^{96}Tc, based on the average value of $\log ft$ for all well-established second-forbidden nonunique transitions [2]. For ^{144}Pm, however, the relevant β^+ decay is a third-forbidden non-unique transition, and there was only one transition of similar forbidenness on which to base the β^+ half-life. Accordingly, the half-life estimates for Pm were too uncertain to permit any conclusions about the suitability of Pm as a cosmic ray clock. The current experimental limits on the β^+ partial half-lives of ^{143}Pm and ^{144}Pm are an order of magnitude lower than the most conservative lower limits considered by Drach and Salamon. If these half-lives turn out to be (much) longer than the mean confinement time of the cosmic rays, then all the (cosmic-ray) Pm isotopes would be electron-capture-decay-only isotopes and their abundance could then be used as a probe of cosmic-ray acceleration and of density variations of the medium traversed by the cosmic rays [1]. Prompted by these considerations, we have attempted to improve on the current experimental limits on the β^+ branches of ^{143}Pm and ^{144}Pm.

II. EXPERIMENTAL PROCEDURE

A. Source preparation

The ^{143,141}Pm source was produced by bombarding a 0.25-mm-thick Pr foil with a beam of 30-MeV α particles from Lawrence Berkeley Laboratory's 88-Inch Cyclotron. The beam

current was 4 μA and the duration of the bombardment was 5 hours. In order to remove positron-emitting contaminants from the source, two weeks after the irradiation the target was dissolved in concentrated HCl; a few drops of concentrated HNO_3 were added and the solution was passed through an anion exchange column of AG1-X8 resin. The Pm was precipitated from the resulting solution with HF. The precipitate was placed inside a well in a plastic planchet. It was dried out under a heat lamp and sealed with tape. This holder insured that any positrons emitted in the decay of ^{143}Pm and ^{144}Pm stopped and annihilated in the source. Two samples were prepared, one which was counted at that point, and another which was counted approximately three years later.

The setup and procedure for the two sets of measurements were very similar. Here we give the details of the experimental procedure for the last set of measurements.

B. Decay rate measurements

The decay schemes of ^{143}Pm and ^{144}Pm are shown in Figs. 1 and 2, respectively. For ^{143}Pm we sought to measure the positron decay rate to the ground state by recording coincidences between the back-to-back 511 keV annihilation photons; for ^{144}Pm we sought to measure the β^+ decay rate of ^{144}Pm to the 697-keV state of ^{144}Nd [5] by recording coincidences between the back-to-back 511-keV annihilation photons and the 697-keV γ ray. A schematic view of the detector arrangement for determining the coincidence rates is shown in Fig. 3. The source was placed between two high-purity Ge (Gamma-X) detectors placed face to face, a distance of $\approx$ 1 cm apart. Each detector had a 52-mm diameter, 57-mm depth and a 3-mm window-to-endcap distance. Both detectors had 0.5 mm Be windows. The Ge detectors were positioned at the center of an 8.25-cm hole in a 30-cm$\times$30-cm NaI detector that was optically divided into two halves. This arrangement gave us the option of recording the 511-511 coincidences in the two Ge detectors, with the 697-keV γ detected in either half of the NaI detector (511_{Ge}-511_{Ge}-697_{NaI}), or recording them in the two halves of the NaI detector, with the 697-keV γ detected in either of the Ge detectors (511_{NaI}-

511_{NaI}-697_{Ge}). As we demonstrate in the next section, the limiting factor for the ^{144}Pm measurement was the number of coincidences between the continuum signals that fall in the 511-511-697 region in each of the detectors. Because of the superior resolution of the Ge detectors (compared to the NaI detector), the number of such "background" coincidences was much smaller for the arrangement 511_{Ge}-511_{Ge}-697_{NaI} than it was for 511_{NaI}-511_{NaI}-697_{Ge}. Thus the 511_{Ge}-511_{Ge}-697_{NaI} configuration proved to be the more sensitive, despite its lower efficiency.

To reduce the count rate due to Nd x, rays a 1-mm Cu absorber was placed in front of each of the Ge detectors. The attenuation of Nd x rays also prevented the summing of the 477-keV γ ray (with the Nd x rays) into the 511-keV gate. To reduce coincidences due to γ ray scattering from one detector into another, 3-mm-thick Pb sheets were wrapped around the Ge detectors and placed in between them.

A standard circuit was used to generate coincidence signals. The energy and fast timing signals from each detector were digitized and recorded event-by-event on magnetic tape for later analysis. To reduce the number of accumulated tapes and dead time associated with data acquisition, only Ge-Ge and Ge-Ge-NaI coincidences were recorded. Counting with the source in the above configuration was carried out for 14.5 days; after that period the source was removed and background was counted for 6.8 days.

The efficiency of the system for detecting back-to-back 511-keV photons and 511-511-697 coincidences was determined using calibrated ^{22}Na, ^{60}Co, and ^{137}Cs sources. In addition to relying on absolutely calibrated sources, the efficiency of each detector for the ^{144}Pm γ rays was also determined from the ratio of triple to double coincidence rates. Summing effects, angular correlation effects, and self absorption in the source were taken into account in all of the above. The resulting efficiency for 511-511 coincidences was $(1.37 \pm 0.12)\%$, and that for 511-511-697 coincidences was $(0.389 \pm 0.034)\%$.

The absolute decay rates of the ^{144}Pm and ^{143}Pm activities were determined in a separate singles run with the source at a distance of $\approx$15 cm from the detector. Figure 4 shows a sample singles spectrum of the source. For these singles runs the efficiency of the detector

was obtained using calibrated ^{133}Ba, ^{60}Co and ^{152}Eu sources. At the start of the last set of coincidence measurements the activity of ^{144}Pm was (0.180 ± 0.005) μCi and that of ^{143}Pm was (0.526 ± 0.032) μCi. For the first set of measurements the activity of ^{144}Pm was (1.4 ± 0.1) μCi and that of ^{143}Pm was (8.1 ± 0.5) μCi.

III. DATA ANALYSIS AND RESULTS

The magnetic tapes were replayed to generate five two dimensional (2D) coincidence histograms: (1) NaI-Ge gated by 511-keV γ rays (detected in the other Ge detector), (2) NaI-Ge gated by 618-keV γ rays, (3) NaI-Ge gated by 697-keV γ rays, (4) Ge-Ge, and (5) Ge-Ge vetoed by the NaI detector. The energy signals from each half of the NaI detector were gain matched so that a signal in either half could be added into the same histogram. The NaI-Ge histograms required a signal in one (and only one) of the NaI halves, *i.e.*, each half vetoed the other, in order to reduce the contribution of Compton scattering and events in which more than three γ rays were produced.

From the three NaI-Ge 2D spectra one can project NaI spectra gated by two γ rays (one detected in each of the Ge detectors), one with an energy of 511, 618, or 697 keV, and the other with any desired energy E. Figure 5 shows NaI spectra gated by (a) 511-511- (b) 511-495-, (c) 511-527-, and (d) 618-477-keV γ rays. Figure 5(d) demonstrates the ability to isolate the 697-keV γ ray in the NaI by detecting it in coincidence with accompanying radiation. The spectrum plotted in figure 5(a) shows no conspicuous evidence for the 697-keV γ ray gated by two 511 keV γ rays. The peak at 1274 keV in this spectrum arises from a small $(42 \pm 4$ pCi) ^{22}Na contaminant in the source. The lines below $\approx$ 1000 keV are not associated with two 511-keV γ rays, but rather with the continuum falling within the two 511-keV gates in the Ge detectors (Fig. 4). This is demonstrated by Figs. 5(b) and 5(c), which show that essentially the same lines appear when one of the Ge gates is set, respectively, below and above the 511-keV region. (In contrast, the ^{22}Na 1274-keV peak, which is clearly associated with the two 511-keV γ rays arising from positron decay,

disappears from the spectrum when one of the gates is set off the 511-keV peak.) The continuum in the 511-keV region arises from Comptons of the 697-keV γ ray (Compton edge at 509 keV) and γ rays of higher energy produced in the ^{144}Pm decay, and from the summing of the 477-keV or the 618-keV γ ray with the Comptons of any of the other γ rays produced in the cascade.

To separate NaI signals in coincidence with true 511-keV γ rays from those in coincidence with the continuum in the 511-keV gate range the following procedure was followed: for each NaI energy (channel) E_{NaI} in the NaI-Ge 2D spectrum gated by 511's a Ge spectrum was projected. The 511-keV peak in each of these spectra was fitted with a Gaussian plus background function. The peak area extracted from each such fit then represents the number of true 511-keV γ rays in coincidence with a signal within the 511-keV gate in the other Ge detector and a signal at energy E_{NaI} in the NaI detector. These yields are plotted as a function of E_{NaI} in Fig. 6 (filled squares with error bars). For comparison, the figure also shows the spectrum obtained by simply setting 511-511 gates (open circles), and a spectrum obtained from a ^{22}Na calibration source and normalized to the same area of the 1275-keV peak. The area of the 697-keV peak in the NaI spectrum in true coincidence with 511-511 coincidences was extracted from a fit using a Gaussian plus a linear background shape. The width and position of the Gaussian was fixed to the result of a fit to the 697-keV peak obtained in coincidence with 477-618-keV Ge coincidences [Fig. 5(d)]. The data and the resulting fit are shown in Fig. 7. The area of the fitted peak was 27 ± 35 counts. After correcting for a small number of accidental coincidences, and for deadtime and pileup losses, the extracted area of triple 511-511-697 coincidences translates to a β^+ branch for ^{144}Pm of $(0.9 \pm 1.3) \times 10^{-4}\%$.

The β^+ branch for ^{143}Pm was deduced from the number of 511-511 coincidences recorded in the Ge detectors, vetoed by the NaI detector. These coincidences were mostly due to the fraction ($\approx$ 22%) of β^+-decays of the ^{22}Na contaminant in which the accompanying 1274-keV γ ray escapes detection by both the NaI and Ge detectors. The contribution of these was determined by multiplying the number of 511_{Ge}-511_{Ge}-1274_{NaI} coincidences

obtained for the Pm source by the ratio of vetoed 511_{Ge}-511_{Ge} coincidences to 511_{Ge}-511_{Ge}-1274_{NaI} coincidences obtained for a ^{22}Na source. After correcting for background 511-511 coincidences, accidentals, pileup and deadtime effects, we obtain a β^+ branch of $(4.5 \pm 5.6) \times 10^{-5}$%.

The β^+ branches obtained from this weak source confirm the results obtained from the first set of measurements, which were $< 5.7 \times 10^{-6}$% for ^{143}Pm and $< 8 \times 10^{-5}$% for ^{144}Pm. For ^{143}Pm the limit is determined by background and unvetoed (contaminant) ^{22}Na 511-511 coincidences; since the relative contribution of these was smaller for the stronger source, the extracted limit was correspondingly lower. For ^{144}Pm, on the other hand, the limit is dominated by coincidences between Comptons of γ rays which arise from ^{144}Pm decay (cf. Fig. 6), (*i.e.*, the "background" scales with the source strength) and hence the stronger source did not give a correspondingly lower limit.

IV. DISCUSSION

The limits on the β^+ branches which we have obtained are approximately a factor of 20 lower than the previous limits of Varga *et al.* [6] ($< 10^{-4}$% for ^{143}Pm and $< 2 \times 10^{-3}$% for ^{144}Pm). From the known half-lives and the present set of limits we obtain β^+ partial half-lives of $> 1.3 \times 10^7$ yr for ^{143}Pm and $> 1.2 \times 10^6$ yr for ^{144}Pm. These half-lives are close to the lower limits considered by Drach and Salamon and hence do not change their conclusions in any way, namely that the half-lives are (still) too uncertain to establish Pm as a good cosmic-ray clock, or as an EC-decay-only cosmic-ray element. For ^{143}Pm it might be possible to reduce the current limit by a factor of ≈ 10 by using a stronger source and reducing the concentration of positron-emitting contaminants; a recent measurement in our Laboratory [7], for example, obtained a limit of $< 5.7 \times 10^{-7}$% for ^{54}Mn, an isotope with a decay scheme and half-life close to that of ^{143}Pm. For ^{144}Pm, however, it is unlikely that the limit could be reduced further with our current setup, because the dominant "background" arises from Comptons of γ rays emitted in the decay of ^{144}Pm. An improvement could be

made if an array of Compton-suppressed Ge detectors were made available for long term counting in a low background environment.

ACKNOWLEDGMENTS

This work was supported by the Director, Office of Energy Research, Division of Nuclear Physics of the U.S. Department of energy, under contract No. DE-AC03-76SF00098 (LBL) and contract No. DE-FG05-87ER40314 (TTU).

REFERENCES

[1] J. Drach and M. H. Salamon, Astrophys. J. **319**, 237 (1987).

[2] For a measurement related to the half-life of ^{95}Tc, see M. M. Hindi, B. Sur, K. L. Wedding, D. W. Bardayan, K. R. Czerwinski, M. T. F. da Cruz, D. C. Hoffman, R.-M. Larimer, K. T. Lesko and E. B. Norman, Phys. Rev. C **47**, 2598.

[3] L. K. Peker, Nucl. Data Sheets, **64**, 429 (1991).

[4] J. K. Tuli, Nucl. Data Sheets, **56**, 607 (1989).

[5] Although decay to the ^{144}Nd ground state is energetically allowed, the transition is fifth forbidden and would be much weaker than the third-forbidden transition to the 697-keV level.

[6] D. Varga, D. Berenyi, C. Ujhelyi and F. Molnar, Nucl. Phys. **A91**, 157 (1967).

[7] M. T. F. da Cruz *at al.*, Phys. Rev. C **48**, 3110 (1993).

FIGURES

FIG. 1. Decay scheme of ^{143}Pm (from Ref. [3]). Level energies are in keV.

FIG. 2. Decay scheme of ^{144}Pm (from Ref. [4]). Level energies are in keV. The weak (6×10^{-4}%) 1396-keV line from the 2093 (5^-) to the 697 (2^+) states is not shown.

FIG. 3. Schematic view of the experimental setup.

FIG. 4. A sample singles spectrum of the ^{143,144}Pm source.

FIG. 5. Spectra recorded in the NaI detector, in coincidence with gamma rays in each of the two Ge detectors. The gamma ray energies in the Ge detectors are (in keV): (a) 511-511, (b) 511-495, (c) 511-527, and (d) 477-618.

FIG. 6. Comparison of NaI Pm spectra obtained by setting 511-511 gates in the Ge (open circles) and subtracting the contribution of continuum in one of the 511 gates, as described in the text (solid squares with error bars). The solid line is a 511-511-gated NaI spectrum for a ^{22}Na source, normalized to the same area of the 1274-keV peak as in the Pm spectra.

FIG. 7. The 697-keV region of the NaI spectrum in coincidence with true 511-511 Ge coincidences (data points) and the Gaussian-plus-background fit (solid line).

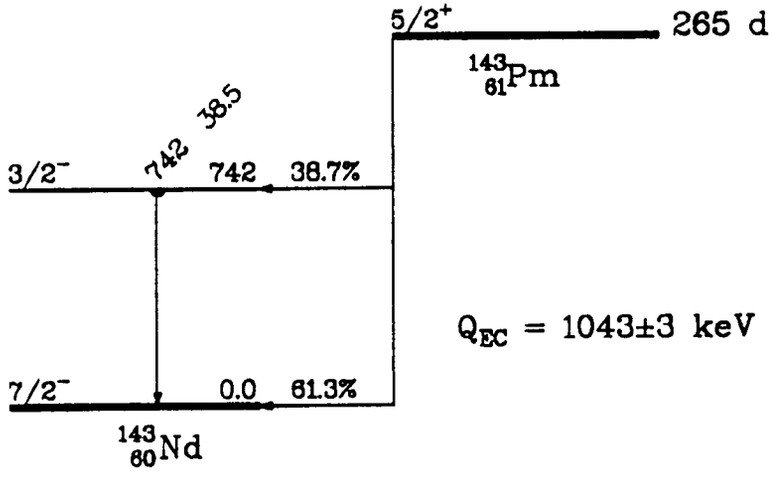
5/2+
265 d
143 61Pm
38.5
742
3/2−
742
38.7%
QEC = 1043±3 keV
7/2−
0.0
61.3%
143 60Nd

Fig 1

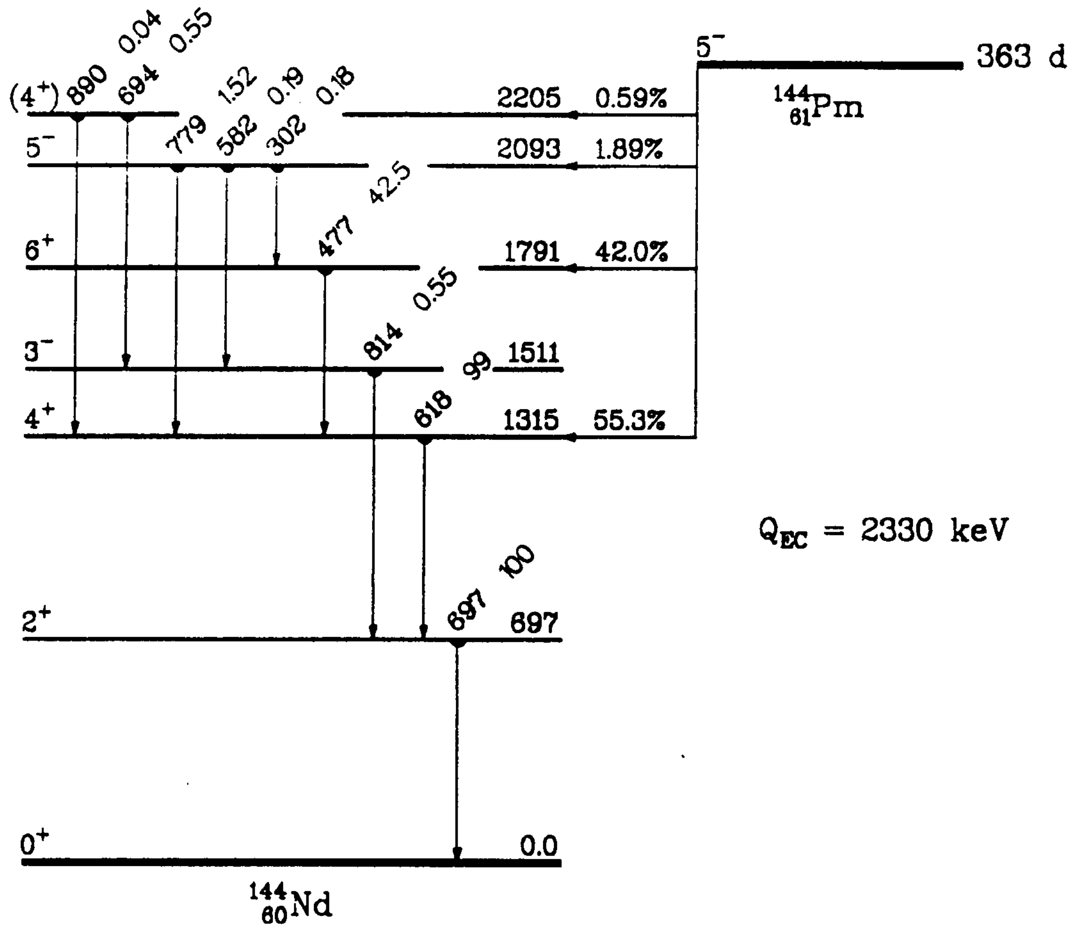

5⁻
363 d
144 61 Pm
Q_EC = 2330 keV
(4⁺)
5⁻
6⁺
3⁻
4⁺
2⁺
0⁺
2205 0.59%
2093 1.89%
1791 42.0%
1511
1315 55.3%
697
0.0
890 0.04
694 0.55
779 1.52
582 0.19
302 0.18
477 42.5
814 0.55
618 99
697 100
144 60 Nd

Fig 2

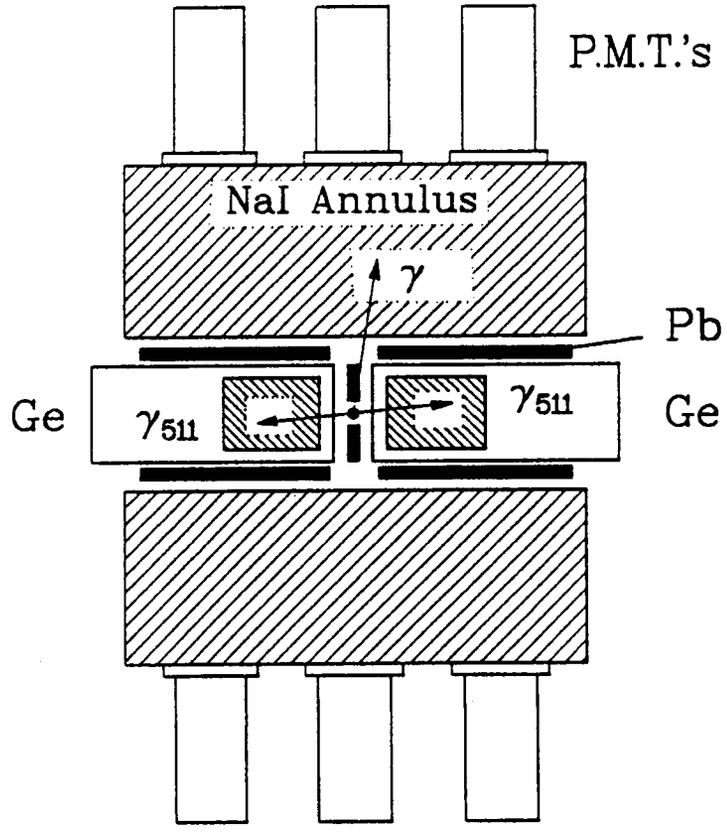

Fig 3

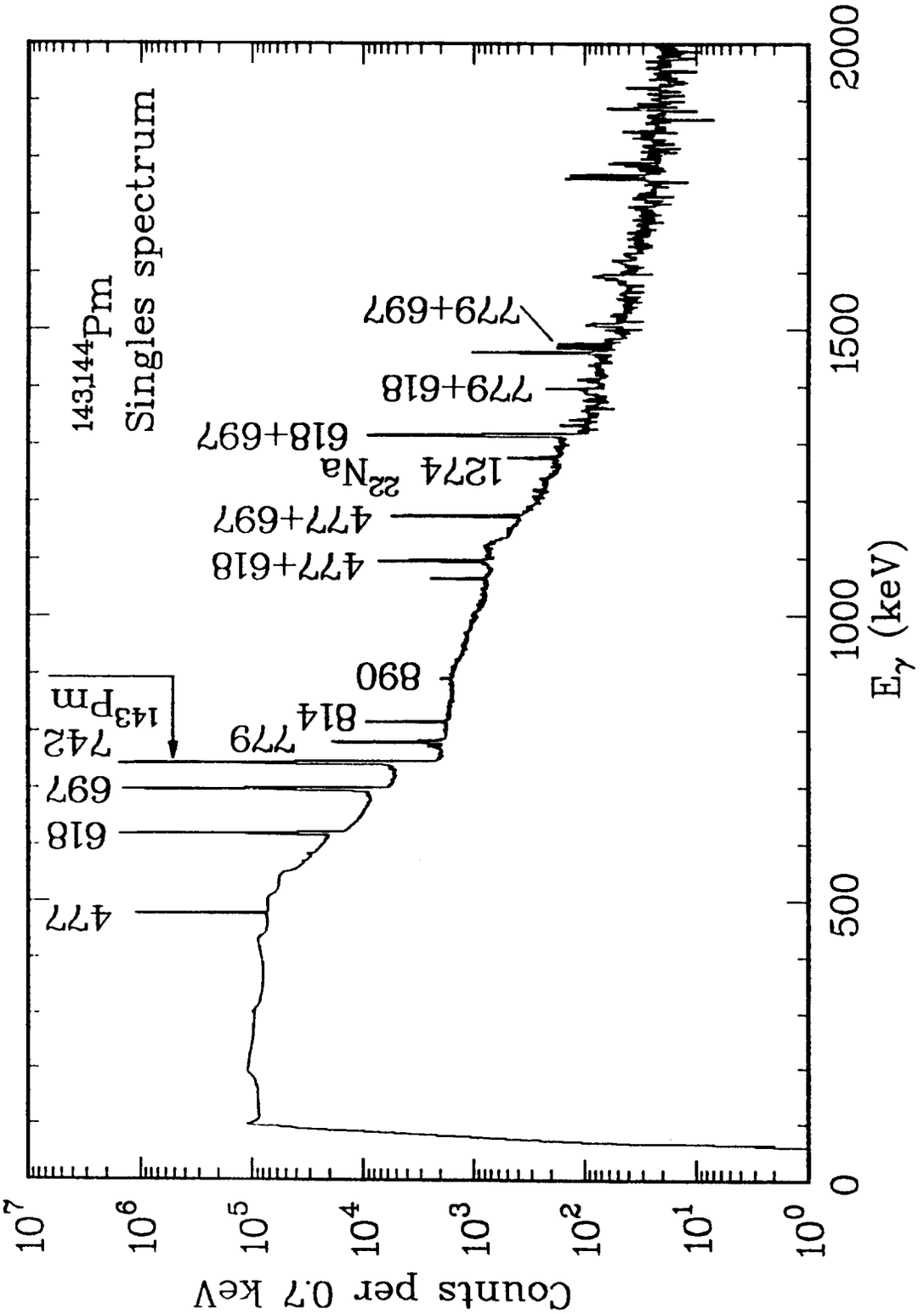
Counts per 0.7 keV
10^7
10^6
10^5
10^4
10^3
10^2
10^1
10^0
0
500
1000
1500
2000
E_γ (keV)
$^{143}_{144}$Pm
Singles spectrum
477
618
697
742
^{143}Pm
779
814
890
477+618
477+697
1274 ^{22}Na
618+697
779+618
779+697

Fig 4

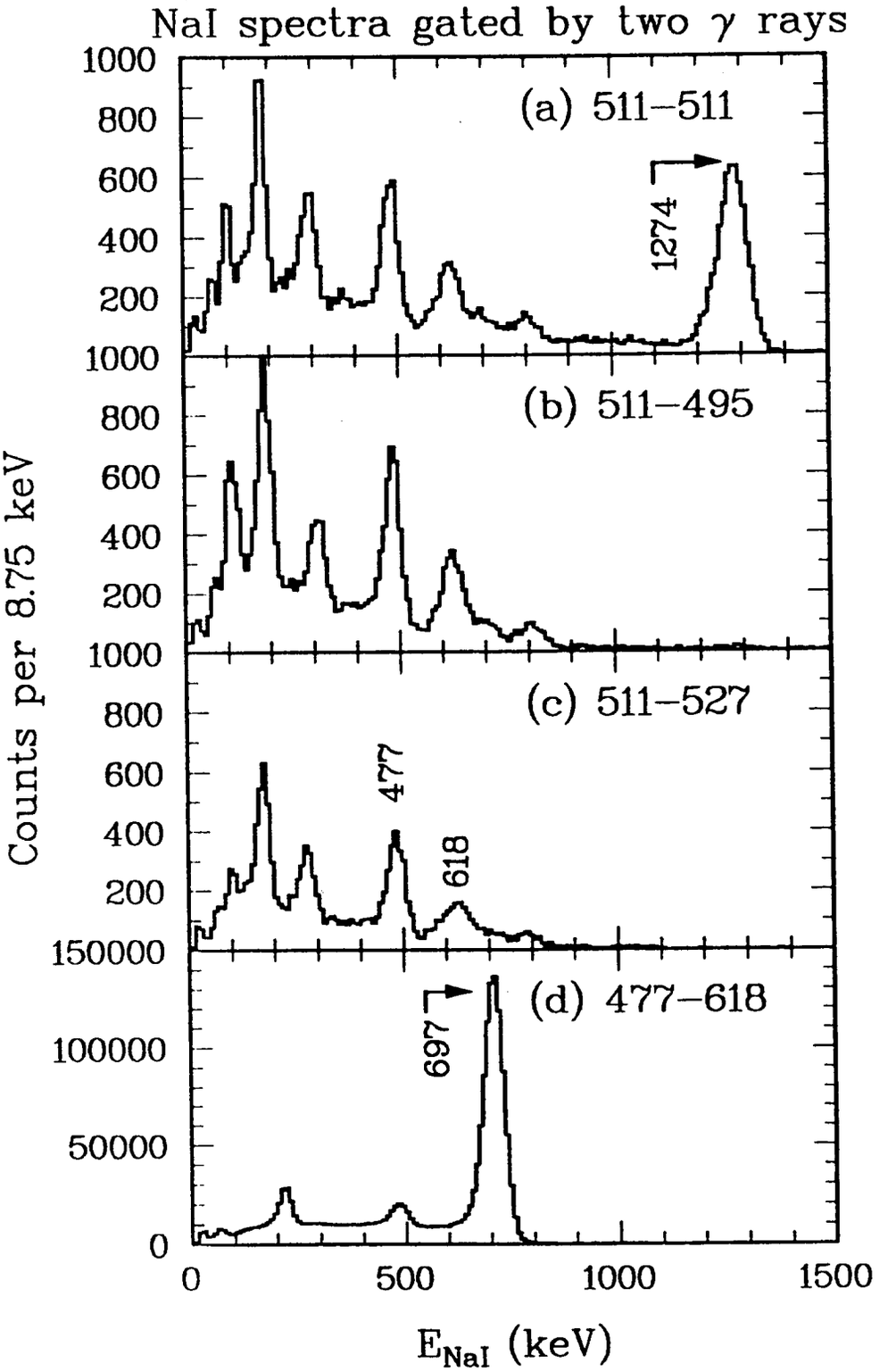
NaI spectra gated by two γ rays
(a) 511–511
1274
(b) 511–495
(c) 511–527
477
618
(d) 477–618
697
Counts per 8.75 keV
E_NaI (keV)
1000
800
600
400
200
150000
100000
50000
0
500
1000
1500

Fig 5

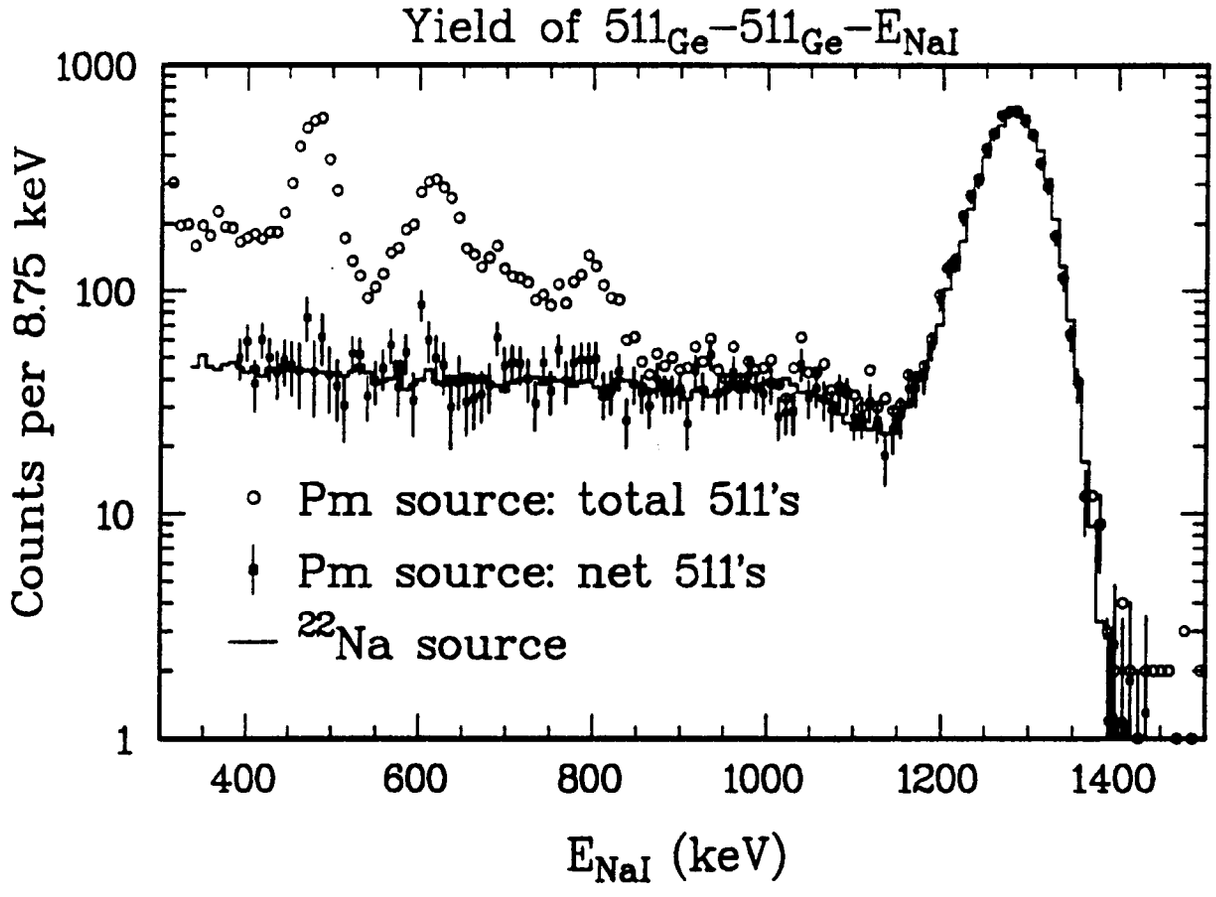
Yield of $511_{Ge}-511_{Ge}-E_{NaI}$
Counts per 8.75 keV
1000
100
10
1
400
600
800
1000
1200
1400
E_{NaI} (keV)
Pm source: total 511's
Pm source: net 511's
^{22}Na source

Fig 6

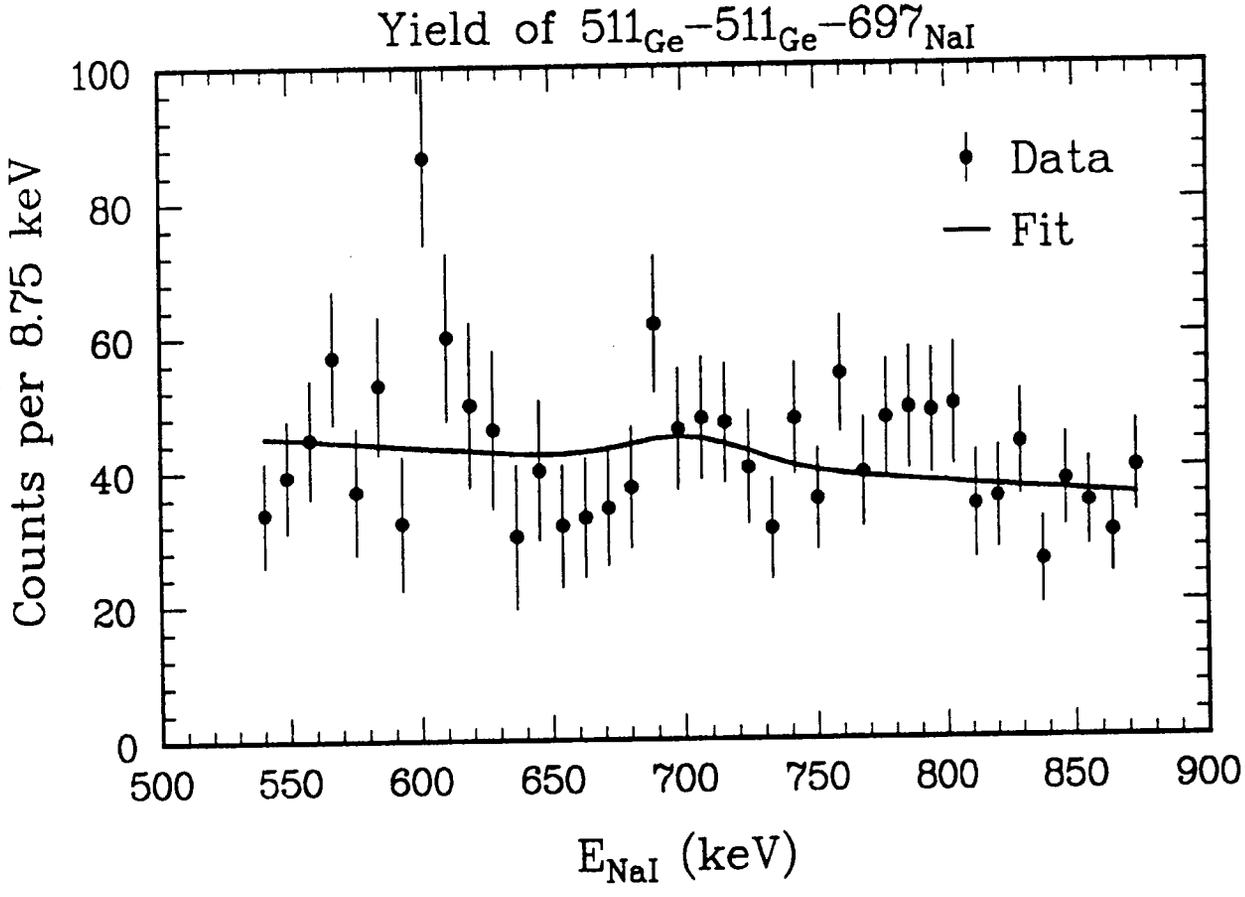
Yield of $511_{Ge}-511_{Ge}-697_{NaI}$
Counts per 8.75 keV
E_{NaI} (keV)
Data
Fit
0
20
40
60
80
100
500
550
600
650
700
750
800
850
900

Fig7